Molecular Crystals and Liquid Crystals Science and Technology. Section A. Molecular Crystals and Liquid Crystals

Publication details, including instructions for authors and subscription information:
http://www.tandfonline.com/loi/gmcl19

# Excitonic and Molecular Properties of the Triplet $T_1$-State in Diphenylpolyene Single Crystals

V. Weiss [a], H. Port [a] & H. C. Wolf [a]

[a] Physikalisches Institut der Universität Stuttgart, Pfaffenwaldring 57, 70550, Stuttgart, Germany

Version of record first published: 04 Oct 2006

To cite this article: V. Weiss, H. Port & H. C. Wolf (1997): Excitonic and Molecular Properties of the Triplet $T_1$-State in Diphenylpolyene Single Crystals, Molecular Crystals and Liquid Crystals Science and Technology. Section A. Molecular Crystals and Liquid Crystals, 308:1, 147-178

To link to this article: http://dx.doi.org/10.1080/10587259708045102

*Mol. Cryst. Liq. Cryst.*, 1997, Vol. 308, pp. 147–178
Reprints available directly from the publisher
Photocopying permitted by license only





# Excitonic and Molecular Properties of the Triplet $T_1$-State in Diphenylpolyene Single Crystals

V. WEISS, H. PORT and H. C. WOLF

*3. Physikalisches Institut der Universität Stuttgart, Pfaffenwaldring 57*
*70550 Stuttgart, Germany*

*(Received 22 July 1997)*

Excitonic properties of the excited triplet state in single crystals of diphenylpolyenes all-trans(1, 4-diphenyl)-1, 3-butadiene (DPB) and all-trans(1, 6-diphenyl)-1, 3, 5-hexatriene (DPH) are derived from $T_1 \leftarrow S_0$ photoexcitation spectra at low temperatures.

The 0-0-transition is split into 2 (DPH monoclinic) and 4 (DPB orthorhombic) Davydov components in zero-field. Measurements with an applied external magnetic field made accessible the respective fine-structure components and their assignment to the principal axes of the fine-structure tensor. In the case of DPB orthorhombic the determination of the excitonic $D^*$ and $E^*$ fine-structure parameters was possible due to the small linewidths occuring in the spectra.

The intensity ratios of the Davydov components were evaluated for different polarizations of the excitation light with respect to the crystal axes. The conclusion is drawn that in both DPH and DPB the transition moment is oriented mainly perpendicular to the molecular plane and that the total symmetry of the $T_1$-state is $A_u$.

The vibrational structure in the photoexcitation spectra was assigned by using selectively deuterated crystal samples for comparison. Since the vibrations involving the phenyl endgroup are absent in the spectra of DPH and carry only very weak intensity in the spectra of DPB it is concluded that the $T_1$-excitation energy is localized mainly on the polyene chain.

*Keywords:* Short-chain diphenylpolyenes; excitonic properties

## 1. INTRODUCTION

Many experimental and theoretical papers have appeared concerning the properties of the lowest excited singlet states of diphenylpolyenes [1, 2]. The chain-length dependence of polyenic molecules is relevant in biophysics and

for synthetic macromolecular systems. Recently diphenylpolyenes also have attracted attention because of their non-linear optical properties [3].

The excited singlet states of short-chain diphenylpolyenes are easily accessible due to the high fluorescence quantum yield. On the other hand little is known about the triplet state as the $T_1 \leftrightarrow S_0$ transition is optically forbidden and phosphorescence cannot be observed.

In an earlier paper [4], preliminary measurements on the triplet state $T_1$ in diphenylhexatriene (DPH) were reported using photoexcitation spectroscopy on single crystals at low temperatures. The spectra indicated the excitonic nature of the triplet state in both crystalline phases of DPH.

In the present work we have extended these studies to diphenylbutadiene (DPB). A comparative more detailed analysis on DPB and DPH was performed with respect to 0-0 transitions (Davydov splittings) and vibrational structures. Excitonic fine-structure was studied in polarized light and applied external magnetic field. Moreover molecular properties of the triplet excited state were investigated, in particular the orientation of the transition dipole and the possible localization of the triplet state on one of the molecular subunits, ring or polyene chain, respectively.

## 2. CRYSTALS

The diphenylpolyenes DPB and DPH can crystallize in two different phases dependent on the growth conditions [5]. They crystallize from ethyl acetate and from acetone in flat monoclinic platelets (thickness $\ll 0.1$ mm). When sublimed in vacuum, the crystals are orthorhombic with a thickness which varies from 0.1 mm to 3 mm. Complete structural data from X-ray analysis are available in the literature for DPH orthorhombic [6]. Data for DPB orthorhombic and DPH monoclinic kindly have been provided by S. Henkel and J. J. Stezowski. The detailed crystal structure of DPB monoclinic is still unknown. Crystal twinning has prevented the X-ray analysis up to now.

Starting material of DPB and DPH has been purchased from Aldrich or Fluka and purified by different methods. The highest purity is obtained using the HPLC itself as purification method. For growing orthorhombic crystals we have used the method of zonemelting as purification method because the amount of purified material obtained by HPLC was not sufficient. There is no difference in the measured spectra of monoclinic crystals when using the first or latter purification method. Both triplet excitation and singlet fluorescence spectra are identical. The solvents used

for growing monoclinic crystals were of spectroscopic grade (Merck Uvasol).

For the DPH *monoclinic* crystal the arrangement of the two differently oriented molecules in the unit cell is shown in Figure 1a. The molecules are arranged in such a way that the axes through the *C*-atoms, linking the phenyl rings with the chain, lie parallel in the *ac*-plane and approximately bisect the monoclinic angle $\beta$. The *b*-axis is perpendicular to these axes.

As a general problem the long axes of diphenylpolyenes are not exactly defined due to the point symmetry of the molecules. This will cause problems discussed in chapter 5 where an exact choice of the axes is needed to calculate intensity ratios.

The least-square-fit planes of the two differently oriented DPH molecules defined by the rings and the chain form an angle of about 60 degrees between each other. The plane of thin crystal platelets matches with the *bc*-plane. The crystal data are given in Table I.

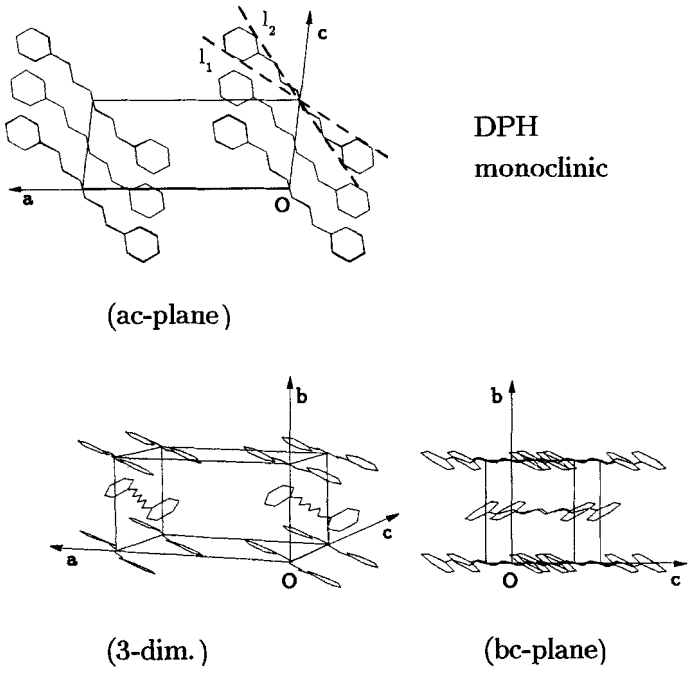


FIGURE 1 Orientation of the molecules in the unit cell of (a) DPH monoclinic and (b) DPB orthorhombic single crystals and projections (a) on the *bc*- and *ac*-plane and (b) on the *ab*- and *ac*-plane; schematically illustrated are the possible choices of molecular axes (region between $l_1$ and $l_2$, see chapter 2).

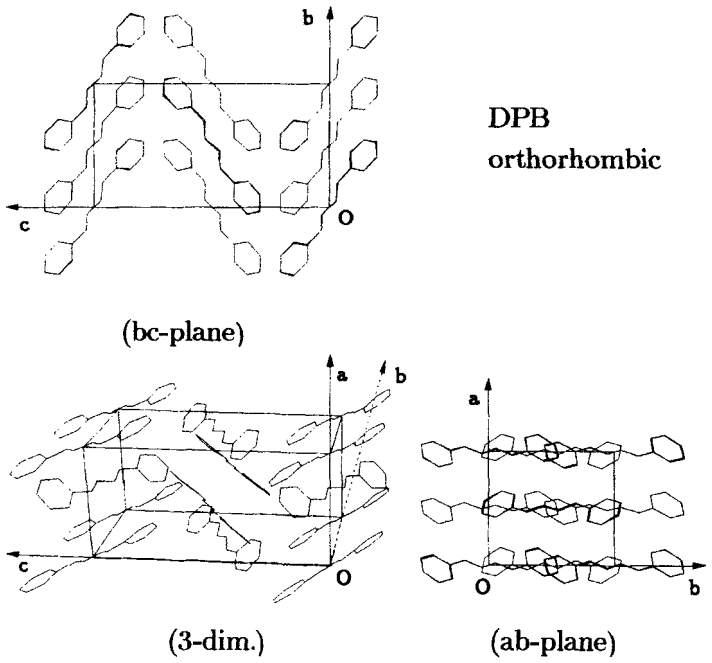


FIGURE 1 (Continued).

TABLE I Crystallographic data of DPH monoclinic and DPB orthorhombic crystals

| | *DPH mono.* | *DPB ortho.* |
|---|---|---|
| *a* | 14.572 Å | 8.243 Å |
| *b* | 7.441 Å | 8.877 Å |
| *c* | 6.250 Å | 16.786 Å |
| $\beta$ | 96.783 ° | 90.000 ° |
| *n* | 2 | 4 |
| $\rho$ | 1.145 g/cm$^3$ | 1.114 g/cm$^3$ |
| spacegroup | $P2_1/c$ | $P_{bca}$ |

The *DPB orthorhombic* crystal contains four molecules in the unit cell (Fig. 1b) and resembles that of DPH orthorhombic [6]. The main difference to DPH monoclinic is that there exist a second pair of molecules with parallel long axes. The axes of the first pair and that of the second pair are not parallel to each other but form an angle of about 70 degrees to each other and an angle of ± 35 degrees to the *b*-axis. All the long axes lie in the

*bc*-plane of the unit cell, so the *a*-axis is perpendicular to these. The crystal data are summarized in Table I.

Crystal quality and optical axes were determined by polarized light microscopy. Using further details given in [5] we were able to assign the principal axes. In the case of DPH monoclinic and DPB orthorhombic we have made Laue measurements in addition which have been compared with calculated Laue spectra to confirm the sample orientation.

In both crystal phases the molecules DPB and DPH are not completely flat but slightly *s*-shaped when viewed from the side. The angle between the plane defined by the phenyl endgroups and that of the polyene chain is about 11 degrees (DPH monoclinic) and 6.5° (DPB orthorhombic). Therefore the actual symmetry is $C_i$ but because we do not know the influence of this slight distortion from an exact plane on the wavefunctions we are treating the diphenylpolyenes in $C_{2h}$ symmetry.

The crystal samples were stored under argon atmosphere in the dark and measured under helium atmosphere.

## 3. EXPERIMENTAL

Photoexcitation spectra were measured using a tunable cw dye laser (Coherent Mod. 599) in standard and narrow band (single frequency) version at a bandwidth of about 1 $cm^{-1}$ and 0.01 $cm^{-1}$, respectively. In this way it was possible to measure lines with a linewidth down to 0.1 $cm^{-1}$. The absolute energetic positions of the laser were determined by a wavemeter. The crystal samples were mounted stressfree in a temperature variable cryostat (4.2 K – 300 K). Photoexcitation was monitored via the delayed fluorescence intensity at selected wavelengths through a double-monochromator or by integral detection through a coloured glass filter (Corning CS 4–96) to block the excitation light. The excitation was kept at low intensity in which limit the delayed fluorescence ($I_{df}$) is proportional to the square of the excitation light intensity ($I_{ex}$). $I_{ex}$ was measured synchronously with the excitation spectra and used for intensity correction afterwards.

The decay time of the delayed fluorescence signal has been measured for DPB orthorhombic with a nitrogen pumped pulsed dye laser. The decay time is about 1 ms which is shorter than the triplet state lifetime measured in solution [7].

The spectra of delayed fluorescence of both crystal phases of DPB and DPH are identical with those of the prompt fluorescence ($S_0 \leftarrow S_1$).

## 4. EXPERIMENTAL RESULTS: SPECTRA AND 0-0 TRANSITIONS

### 4.1. Overall Spectra

In Figure 2 the $T_1 \leftarrow S_0$ photoexcitation spectra of DPB monoclinic and DPB orthorhombic observed at $T = 20$ K are presented. They cover the energy range up to about 1900 $cm^{-1}$ from the respective origins (lines 0 in Fig. 2) to higher energy. The spectra consist of narrow lines (fwhm $< 10$ $cm^{-1}$) and have a similar vibronic structure.

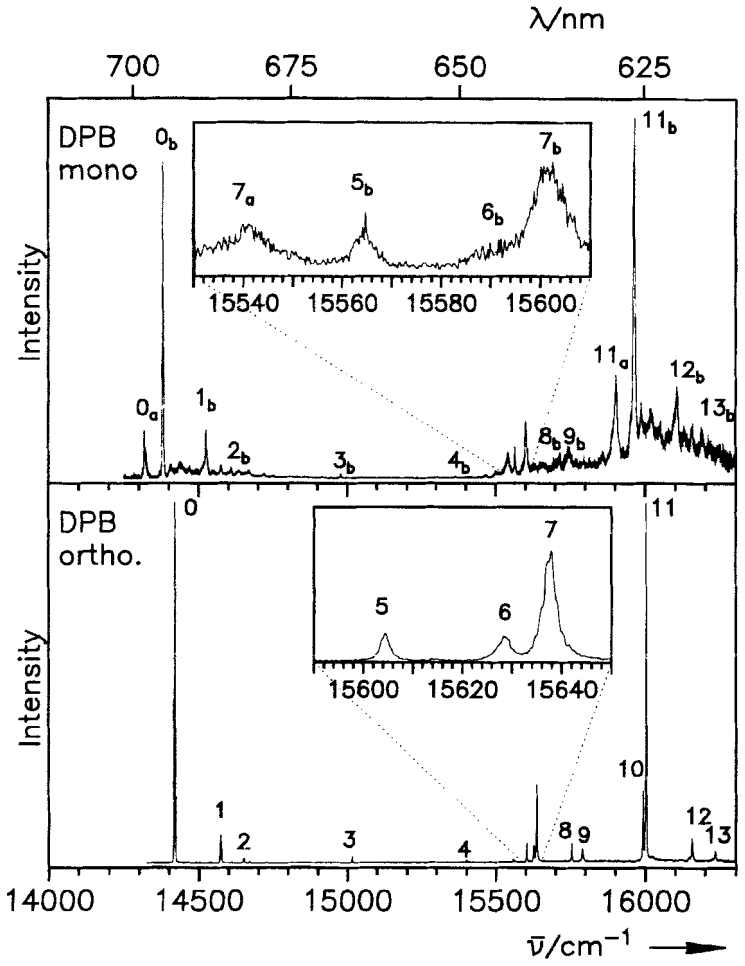


FIGURE 2 Triplet photoexcitation spectra of DPB at $T = 20$ K (a) monoclinic, above; (b) orthorhombic, below; insert: range of C—C vibrations (see Tab. II) in extended energy scale.

For DPB monolinic (Fig. 2a, above) there exist two series of 0-0 transitions and related vibronic lines labelled *a* and *b* with different relative intensities and linewidths. The energetic distance between the two series is 62 $cm^{-1}$.

A similar behaviour is observed in the triplet excitation spectra of stilbene (diphenylethylene) [8] (distance between the two series: 82 $cm^{-1}$) and is attributed to a site splitting. The unit cell of stilbene consists of 4 molecules which are pairwise symmetrical at different sites. Although the complete crystal structure of DPB monoclinic is not resolved, it is known that the number of molecules per unit cell is more than 2. Numbers reported in the literature vary from 4 [9] to 8 [5, 10]. So we suggest that the two different series of lines belong to two different sites of the DPB molecules in the monoclinic crystal.

Instead, the spectrum of DPB orthorhombic (Fig. 2b) consists of a single line series. The origin (line 0) is blue-shifted relative to the origin of series *b* in Figure 2a (DPB monoclinic) by about 38 $cm^{-1}$.

Photoexcitation spectra of both phases of DPH have been reported previously [4]. The energetic positions of the 0-0 transition are lower in energy but the overall appearance of the spectra resembles that of DPB orthorhombic. Therefore the vibrational assignment for the DPB spectra given in Table II will be discussed in Chapter 6 in comparison with the results on DPH and new data on deuterated DPH.

TABLE II Energetic positions of the lines in the measured triplet photoexcitation spectra of DPB monoclinic and DPB orthorhombic at $T = 20$ K (see Fig. 2); in absolute wavenumbers (0-0 transition) and relative wavenumbers (vibrations)

| *line No.* | *DPB mono.* | | *DPB ortho.* | *assignment* |
|---|---|---|---|---|
| | *a* | *b* | | |
| 0 | 14321/14383 | | 14421 | 0-0 transition |
| 1 | 144 | | 156 | $\nu_{29}$ [*)1] |
| 2 | 226 | | 230 | $\nu_{28}$ [*)1] |
| 3 | 595 | | 595 | *ring 6a* [*)2] |
| 4 | 980 | | 980 | *ring 1* |
| 5 | 1179/1181 | | 1186 | C—C stretch chain |
| 6 | | | 1211 | C—C stretch chain |
| 7 | 1220/1219 | | 1219 | C—C stretch chain |
| 8 | 1332 | | 1337 | 5 + 1 |
| 9 | 1362 | | 1373 | 7 + 1 |
| 10 | | | 1575 | C=C stretch *ring 8b* |
| 11 | 1580/1580 | | 1585 | C=C stretch *ring 8a* |
| 12 | 1723 | | 1738 | 11 + 1 |
| 13 | 1807 | | 1813 | 11 + 2 |

[*)1] Labelling according to Pierce und Birge [31].
[*)2] Labelling of the *ring* modes according to Wilson [29].

### 4.2. 0-0-Transitions

In the following, we present a detailed analysis of the 0-0 region of the photoexcitation spectra ($T_1 \leftarrow S_0$). In Figure 3 high resolution spectra at $T = 4.2$ K for the 0-0 transitions of the monoclinic and orthorhombic DPB and DPH crystals are shown. The crystals have been measured with the exciting laser beam perpendicular to the developed sample plane. This was the *bc*-plane for the monoclinic crystals and the *ab*-plane for the orthorhombic crystals, respectively (see Chapter 2). Each plot consists of two spectra obtained in two different polarizations of the exciting laser light parallel to the crystal axes.

For *DPB monoclinic*, no splittings or differences in lineshapes in the spectra for $E \parallel b$ and $E \parallel c$ appear. As an example in Figure 3 the case of the narrower 0-0 line (line Ob, fwhm: 3.5 $cm^{-1}$) is shown for different polarizations.

For *DPH orthorhombic* a splitting of the 0-0-transition is indicated but the two line components could not be clearly resolved despite of a much narrower linewidth. Both, the absolute and the relative intensities of the two observable components are different for $E \parallel a$ and $E \parallel b$.

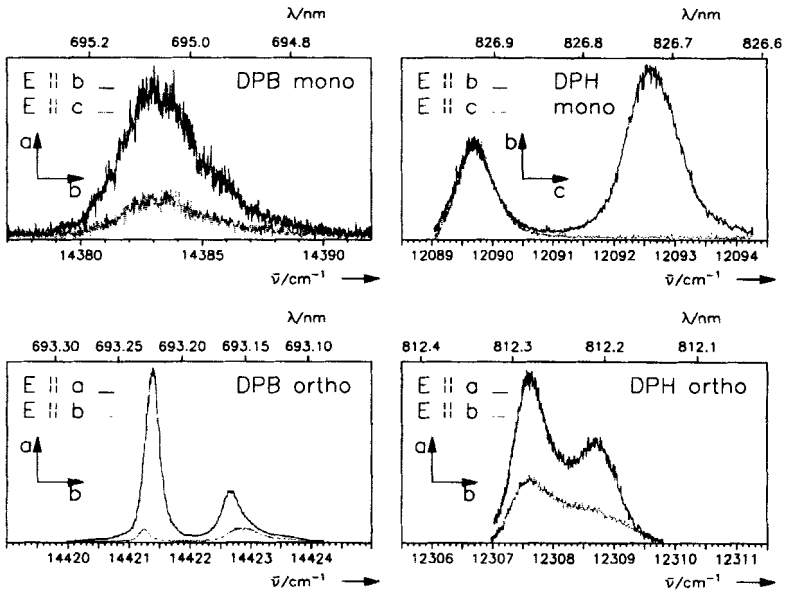


FIGURE 3 0-0 region of triplet photoexcitation spectra for both crystal phases (monoclinic and orthorhombic) of DPB and DPH for different polarizations of the exciting light at $T = 4.2$ K; monoclinic: $E \parallel b$ (full line), $E \parallel c$ ( dotted), orthorhombic: $E \parallel a$ (full line), $E \parallel b$ (dotted). The energy range is 6 $cm^{-1}$, for DPB monoclinic 15 $cm^{-1}$ (line 0*b*, see Fig. 2).

A competely resolved splitting is observable in the spectra of *DPH monoclinic* and *DPB orthorhombic*. Therefore these two substances allow a more detailed analysis in the next sections.

### 4.3. 0-0-Subcomponents DPB Orthorhombic

The spectra of the 0-0-transition of DPB orthorhombic are seperately plotted in Figure 4 in enlarged energy scale. The spectrum $E \| a$ consists of

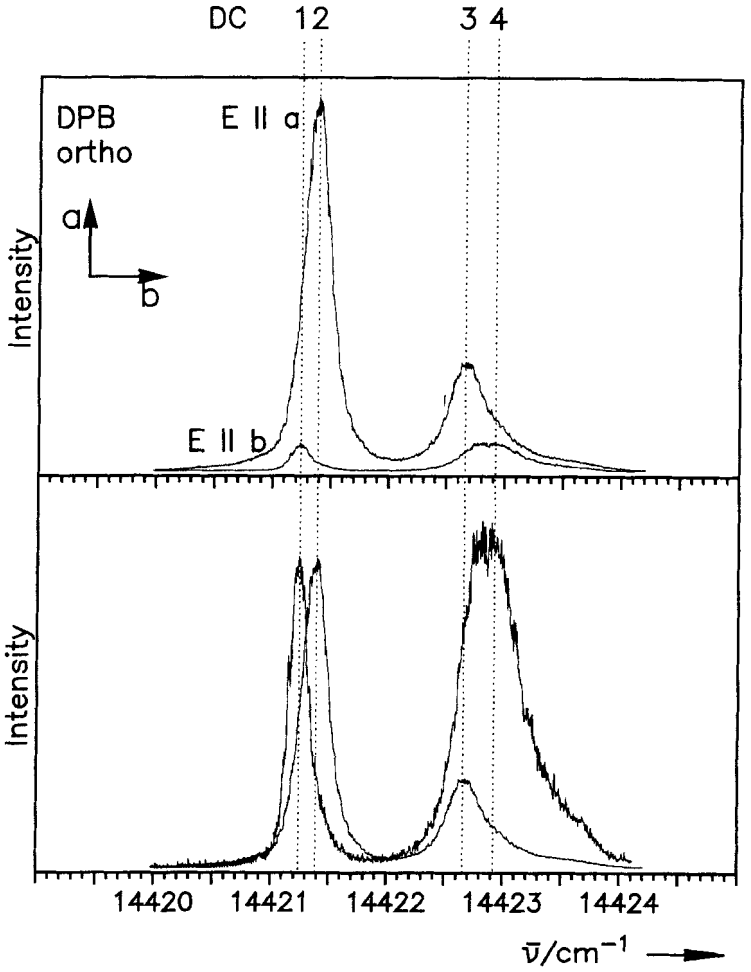


FIGURE 4 0-0 region of the triplet photoexcitation spectra of DPB orthorhombic at $T=$ 4.2 K; polarization of the exciting light $E \| a$ and $E \| b$; absolute intensities in upper traces, normalized intensities in lower traces; distinction of Davydov components DC 1...4, see text.

two lines exhibiting an energy splitting of 1.27 $cm^{-1}$. The line positions are 14421.39 $cm^{-1}$ and 14422.66 $cm^{-1}$, respectively.

Changing the polarization from $E \| a$ to $E \| b$, the total intensity diminishes drastically by a factor of 7.3. Moreover the line positions change in different sense. This is shown in Figure 4 (below) in which both spectra are plotted with normalized intensities. The low energy line is located at 14421.28 $cm^{-1}$, i.e. red shifted with respect to $E \| a$ by 0.11 $cm^{-1}$. The high energy line is blue shifted and has a larger linewidth as compared to that of spectrum $E \| a$. The reason is that this line is a superposition of two components.

A detailed analysis reveals that the spectra $E \| a$, $E \| b$ (and all the other spectra with polarization direction in the *ab*-plane) can be generated by a superposition of 4 lines DC 1...4 with appropriately weighted intensities. Consequently the high energy line in the spectrum $E \| b$ results from a superposition of DC 3 and DC 4. The energetic position of DC 4 is 14422.92 $cm^{-1}$. The lines DC 1...4 are tentatively attributed to the four Davydov components of the 0-0 transition in the triplet photoexcitation spectra of DPB orthorhombic, because their number and discrete polarization behaviour correspond to theoretical expectations as is explained in Chapter 5.1. The energetic positions and linewidths are summarized in Table III.

### *Measurements with an Applied Magnetic Field*

To confirm this assignment and to separate possible further substructures (triplet sublevels of the DC), triplet photoexcitation spectra of the 0-0 transition with an applied static magnetic field have been measured. Corresponding to the two possible directions of the magnetic field parallel to the principal axes ($B \| a$, $B \| b$) and the two different polarizations ($E \| a$,

TABLE IIIa Energetic positions, linewidths (fwhm) and distances of the four Davydov components DC 1... 4 of the 0-0 line of DPB orthorhombic at $T = 4.2$ K (see Fig. 4)

| | *line position* | *fwhm* | *δ* | *δ DC1–DC4* |
|---|---|---|---|---|
| DC1 | 14421.28 $cm^{-1}$ | (0.20 $cm^{-1}$) | | |
| | | | 0.11 $cm^{-1}$ | |
| DC2 | 14421.39 $cm^{-1}$ | (0.27 $cm^{-1}$) | | |
| | | | 1.27 $cm^{-1}$ | 1.64 $cm^{-1}$ |
| DC3 | 14422.66 $cm^{-1}$ | (0.40 $cm^{-1}$) | | |
| | | | 0.26 $cm^{-1}$ | |
| DC4 | 14422.92 $cm^{-1}$ | (0.47 $cm^{-1}$)* | | |

*energetic position and linewidth (fwhm) of DC 4 are obtained by substraction of spectrum $E \| a$ (Fig. 4) from spectrum $E \| b$ with appropriate intensity.

TABLE IIIb Energetic line positions, distances and linewidths of the four Davydov components DC 1...4 of the 0-0 line of DPB orthorhombic at three temperatures: $T = 4.2$ K, $T = 10$ K and $T = 20$ K (see Fig. 6) data given in $cm^{-1}$

| $E \parallel a$ | *DC 2* | $\delta$ | *fwhm* | *DC 3* | $\delta$ | *fwhm* |
|---|---|---|---|---|---|---|
| 4.2 K | 14421.39 | | 0.27 | 14422.66 | | 0.40 |
| | | 0.08 | | | 0.08 | |
| 10 K | 14421.31 | | 0.37 | 14422.58 | | 0.56 |
| | | 0.31 | | | 0.35 | |
| 20 K | 14421.00 | | 1.14 | 14422.23 | | 1.40 |
| $E \parallel b$ | *DC 1* | $\delta$ | *fwhm* | *DC 4** | $\delta$ | *fwhm* |
| 4.2 K | 14421.28 | | 0.20 | 14422.92 | | 0.47 |
| | | 0.07 | | | 0.10 | |
| 10 K | 14421.21 | | 0.29 | 14422.82 | | 0.63 |
| | | 0.27 | | | 0.27 | |
| 20 K | 14420.94 | | 1.20 | 14422.55 | | 1.40 |

*energetic position and linewidth (fwhm) of DC 4 are obtained using a Lorentzian line fit (Fig. 6).

$E \| b$), four different spectra ①, ②, ③ and ④ have been obtained which are shown in Figure 5 for $B = 0.27$ $T$ and for $B = 0$ $T$ as reference. The spectra are analyzed with regard to the linepositions and relative intensities. The essential features of spectra ①...④ are as follows:

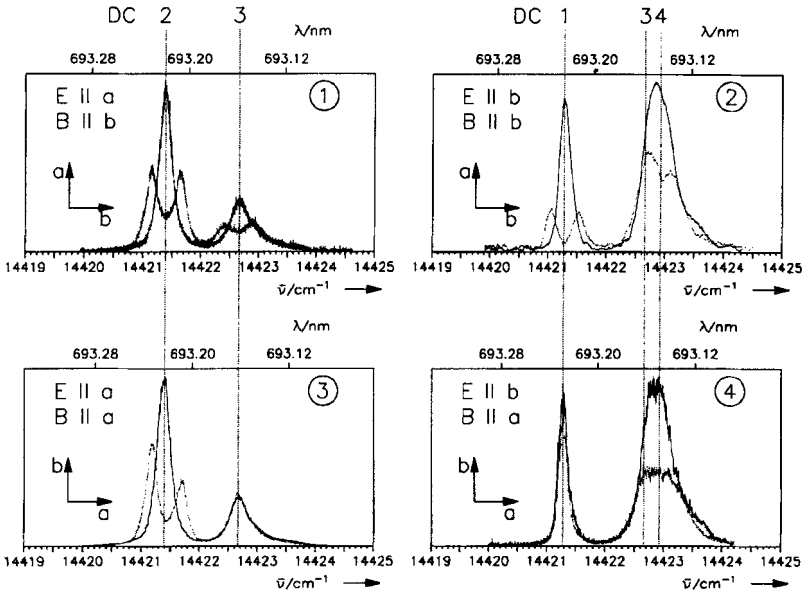


FIGURE 5 0-0 region of the triplet photoexcitation spectra of DPB orthorhombic, magnetic field effect at $T = 4.2$ K; polarization of the exciting light and field orientation are varied. full line: $B = 0$ $T$, dotted line $B = 0.27$ $T$; ①: $E \parallel a$, $B \parallel b$; ②: $E \parallel b$, $B \parallel b$; ③: $E \parallel a$, $B \| a$; ④: $E \parallel b$, $B \| a$.

For $E \| a$ (spectra ① and ③), DC 2 splits into two Zeeman components for both $B \| b$ and $B \| a$ whereas DC 3 is split only for $B \| b$. The amount of the splitting is about 0.5 $cm^{-1}$ in all cases. The relative intensities of the Zeeman components are equal for DC 2, $B \| b$, but different for DC 2, $B \| a$, and DC 3, $B \| b$.

For $E \| b$ (spectra ② and ④), the Zeeman splitting is clear-cut only for DC 1, $B \| b$, but less pronounced for the superposition of DC 3 and DC 4. For $B \| a$, DC 1 is not affected by the magnetic field similarly as DC 3 in ③.

### *Temperature Dependencies*

In Figure 6, the spectra of the 0-0-transition are given at three different temperatures ($T = 4.2$ K, 10 K and 20 K) for polarizations $E \| a$ and $E \| b$, respectively. With increasing temperature all the lines DC 1... DC 4 are red shifted by slightly different amounts and the linewidths are broadened (see Tab. III). At $T = 20$ K, the line components are no longer spectrally resolved. Therefore a Lorentzian line fit was applied to determine the energetic positions and linewidths.

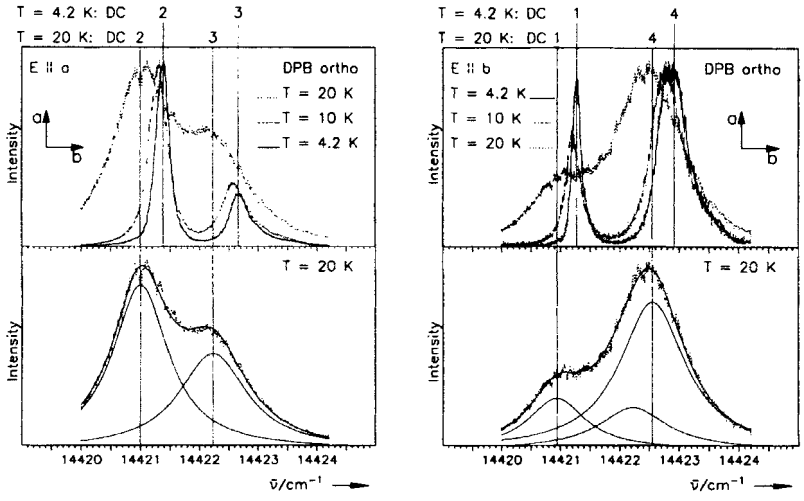


FIGURE 6 0-0 region of the triplet photoexcitation spectra of DPB orthorhombic at different temperatures and for polarization of exciting light $E \| a$ (left) and $E \| b$ (right). Curves above: $T = 4.2$ K, 10 K and 20 K, respectively; curves below: $T = 20$ K with Laurentzian line fit (see text).

### 4.4. 0-0-Subcomponents DPH Monoclinic

The 0-0 transtion in the spectra of DPH monoclinic (Fig. 3) shows a splitting into two components in zero field, located at 12089.7 $cm^{-1}$ and 12092.6 $cm^{-1}$, respectively. These are tentatively attributed to the expected two Davydov components DC 1 and DC 2 (see Chapter 5.1). The energy difference of the two components is 2.9 $cm^{-1}$. Remarkably the linewidth (fwhm) of the low energy component DC 1 is smaller than of DC 2 (DC 1: 0.6 $cm^{-1}$, DC 2: 0.9 $cm^{-1}$). For $E \| c$, DC 2 is totally absent, which reflects its pronounced polarization behaviour. DC 1, instead, remains unchanged in intensity and linewidth.

#### *Measurements with an Applied Magnetic Field*

In Figure 7, the spectra ①... ⑥ of the 0-0 transition are shown for different orientations of the crystal relative to the magnetic field at $B = 0.34\,T$ together with the spectra at zero field as reference.

In contrast to the spectra of DPB orthorhombic no splitting is observable in the spectra of DPH monoclinic with an applied magnetic field due to the larger linewidths of the Davydov components DC 1 and DC 2. However, distinct intensity changes appear dependent on the magnetic field orientation (Fig. 7). At $B \| c$, spectra ① and ②, the intensities of both DC 1 and DC 2 are influenced but at $B \perp b$ and $B \| b$, spectra ③–⑥, only one component, either DC 1 or DC 2 for different polarizations.

For ③and ④ the crystal was turned around the $b$-axis with respect to the orientation for ①and ②by about 45 degrees. Thus the orientation of the magnetic field was not parallel to a crystal axis anymore but still perpendicular to the $b$-axis. The choice of this particular orientation will be explained in Chapter 5.2.

#### *Temperature Dependence*

Upon increasing the temperature from $T = 4.2$ K to $T = 20$ K, the energetic positions of both components DC 1 and DC 2 are blue shifted – in contrast to the case of DPB orthorhombic – and by different amounts (DC 1: 1.4 $cm^{-1}$; DC 2: 0.6 $cm^{-1}$); in Figure 8 the case of $E \| b$ is given as an example. This leads to a strong reduction of the energy splitting from 2.9 $cm^{-1}$ at $T = 4.2$ K to 2.1 cm at $T = 20$ K. In parallel with the lineshifts the temperature variation also causes a different line broadening for DC 1 and DC 2. As a result the linewidths become equal at $T = 20$ K (fwhm: 1.2 $cm^{-1}$).

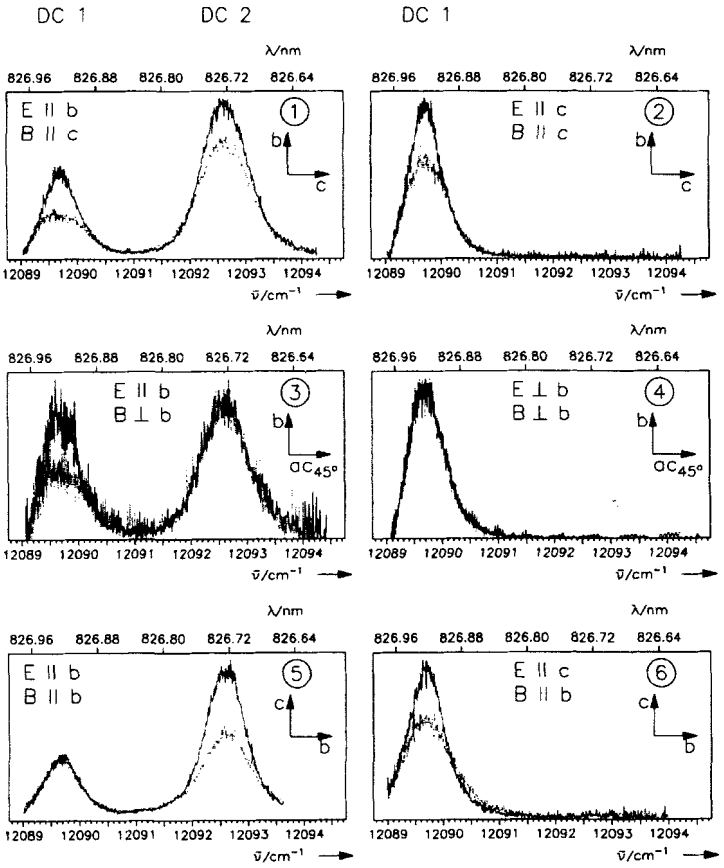


FIGURE 7 0-0 region of the triplet photoexcitation spectra, DPH monoclinic at $T = 4.2$ K for different polarizations of the exciting light and for different orientation of an applied magnetic field $B = 0.34$ $T$ (dotted lines); spectra at $B = 0$ $T$ (full lines) as reference. ①: $E \parallel b$, $B \parallel c$; ②: $E \parallel c$; $B \parallel c$; ③: $E \parallel b$, $B \perp b$; ④: $E \perp b$, $B \perp b$; ⑤: $E \parallel b$, $B \parallel b$; ⑥: $E \parallel c$, $B \parallel b$.

## 5. DISCUSSION: THE 0-0-TRANSITION, DAVYDOV-SPLITTING

The major aim of this chapter is to examine the excitonic properties of the excited triplet state for DPB orthorhombic and DPH monoclinic. In 5.1. the energetic positions, splitting and strong polarization dependence of the 0-0 transitions are discussed in terms of Davydov exciton theory [11]. The assignment of the Davydov components and their fine-structure is verified in 5.2. From the measurements with applied magnetic field. The excitonic fine-structure parameters $D^*$ and $E^*$ are evaluated for DPB orthorhombic. Finally, in 5.3. from the line intensities of the Davydov components in zero

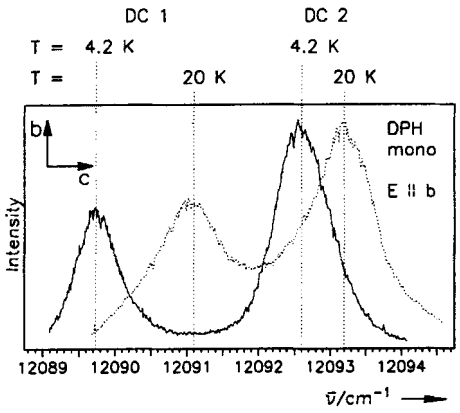


FIGURE 8 0-0 region of the triplet photoexcitation spectra, DPH monoclinic, at different temperatures. $T = 20$ K and $T = 4.2$ K, resp., for $E \parallel b$.

field informations on the molecular transition moment and the symmetry of the molecular triplet $T_1$-state are derived.

### 5.1. 0-0-Energies and Davydov Splittings

It is well known how the molecular electronic states are modified into excitonic states in molecular crystals. In general the excitonic energies are reduced as compared to those of the free molecules due to static interactions (solvent shift) which are essentially larger than the dynamic interactions contributing only in the excited state. As the solvent shifts in crystals are small relative to the absolute energy of the excited states and comparable to those in liquid environment, the order of magnitude of the 0-0 energy can be compared in first approximation with literature data of the molecular 0-0 energy obtained by absorption measurements in liquid solutions [7, 12, 13] and by phosphorescence in zeolites [14].

The energies of the observed $T_1 \leftarrow S_0$ 0-0 transitions in this paper are in agreement with the range of values reported in literature. They exhibit the same chain-length dependence of energetic positions as known from $S_1 \leftarrow S_0$ absorption and emission in polyenic systems [1, 2]. The solvent shift of both diphenylpolyenes is larger in the monoclinic phase than in the orthorhombic phase. This can be attributed to the closer molecular packing in this phase.

The dynamic interaction between translational equivalent and inequivalent molecules determines the excitonic bandwidth and structure. Depen-

ding on the number of molecules per unit cell, excitonic substates (factor group states) are formed, however, optically accessible are only the ($k \approx 0$)-states the so-called Davydov components (DCs).

In the case of *DPB orthorhombic* the crystal symmetry is described by space group $D_{2h}^{15}$ with four molecules per unit cell, located at sites of $C_i$ symmetry (Fig. 1b). It is the same crystal symmetry as found for benzene [15]. The theoretical treatment [16, 17] gives four spatial factor group states $A_u$, $B_{1u}$, $B_{2u}$ and $B_{3u}$ which are representations of the $D_{2h}$ factor group. In the $T_1 \leftarrow S_0$ photoexcitation spectra the transitions in this factor group are expected to be represented by 4 DCs.

The unit cell of *DPH monoclinic* (Fig. 1a) with space group $C_{2h}^5$ consists only of two molecules, located at sites of $C_i$ symmetry. Typical examples for the theoretical treatment of this space group are naphthalene, anthracene and $\beta$-perylene which have been studied in detail [18 – 21]. There are two spatial factor group states to be expected. $T_1 \leftarrow S_0$ transitions in both states are optically symmetry allowed and therefore two DCs are to be expected in the triplet photoexcitation spectra.

The number of 0-0 line components in the experimental spectra (Figs. 3 and 4) agrees with the theoretical expectation, DC 1, 2, 3, 4 for DPB orthorhombic and DC 1 and 2 for DPH monoclinic. Moreover in accordance to theory the DCs are polarized parallel to the crystal axes of DPB orthorhombic and of DPH monoclinic.

The energy splitting of the Davydov components is determined by the relative orientations of the molecules, the intermolecular distances and the overlap of the excitonic wavefunctions which however are not known for the present cases. The observed Davydov splittings are in the order of magnitude found earlier for triplet excitonic states of many other molecular crystals [17 – 19].

The dynamic interactions in the excited state are strongly temperature dependent due to the sensibility of molecular distances to temperature changes. The reduced splitting of the 0-0 transition measured for DPH monoclinic at higher temperatures is caused by the different energy shift of DC 1 and DC 2 and can be taken as a hint for the existence of two dynamic interactions with different temperature dependencies. This result also supports the excitonic nature of the observed 0-0 lines. For trap signals such behaviour would not be expected.

Further support for the existence of highly mobile excitions in both DPB orthorhombic and DOH monoclinic is the high intensity of the delayed fluorescence indicating effective energy trasnport and triplet-triplet annihilation.

### 5.2. Triplet Exciton Sublevels – Fine Structure (*fs*) Splittings

Each spatial factor group state, represented by the DCs in the spectra, consists of three excitonic substates (spin orbit states) obtained from the spatial representations (orbital part) after multiplying by the triplet spin representations. In the case of DPB orthorhombic there exist altogether 12 spin orbit states. Transitions into nine of them are allowed in the electric dipole approximation [16]. The transitions from ground state to the spin orbit states are represented in the spectra by the *fs*-components. In the case of DPH monoclinic all the transitions to the six spin orbit states are allowed and therefore six *fs*-components are to be expected.

All the *fs*-components are strongly polarized parallel to the principal axes of the *fs*-tensor. For DPB orthorhombic these axes are identical with the crystal axes *a*, *b* and *c* of the unit cell. For DPH monoclinic only one *fs*-tensor axis coincides with a crystal axis (*b*-axis). The other is presumed to be located within the *ac*-plane perpendicular to the *b*-axis as shown in Figure 9 and be confirmed using the measurements with an applied external magnetic field as shown below. According to the McConnell convention [22] the *b*-axis is assigned as $z^*$-axis. For DPB orthorhombic we have chosen the convention $c \leftrightarrow x^*$, $a \leftrightarrow y^*$ and $b \leftrightarrow z^*$ for reasons given below when discussing the *fs*-parameters $D^*$ and $E^*$.

The *fs* of triplet excitons has been treated in [22]. It can be described in a way similar to that for isolated molecules by the spin hamiltonian $\hat{H}_s$:

$$\hat{H}_s = D^*\left[\hat{S}^2_{z^*} - \frac{1}{3}S(S+1)\right] + E^*(\hat{S}^2_{x^*} - \hat{S}^2_{y^*}) \tag{1}$$

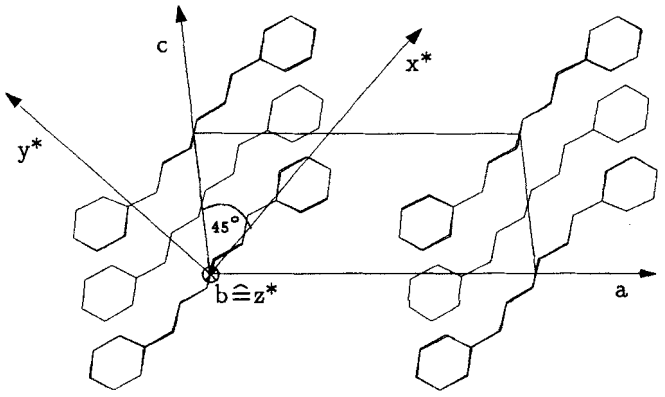


FIGURE 9 Fine structure tensor principal axes for DPH monoclinic. Projection of the molecules in the *ac*-plane. According to McConnell [22] the crystallographic *b*-axis coincides with the $z^*$-axis of the finestructure tensor. $x^*$ and $y^*$ within the *ac*-plane perpendicular to the $z^*$-axis.

Here $D^*$ and $E^*$ are the *fs*-parameters and $\hat{S}_{x^*}, \hat{S}_{y^*}$, und $\hat{S}_{z^*}$ are the components of the spin-operator in the principal axes system of the three zero field spin states whose energy eigenvalues read as:

$$\begin{aligned} t_{x^*} &: E_{x^*} = \frac{1}{3}D^* - E^* \\ t_{y^*} &: E_{y^*} = \frac{1}{3}D^* + E^* \\ t_{z^*} &: E_{z^*} = -\frac{2}{3}D^* \end{aligned} \tag{2}$$

Actually the zero field splitting of the *fs*-components is small relative to the linewidths of the DCs in the spectra of both compounds. Therefore different *fs*-components could not be distinguished in the spectra in zero field (Figs. 3 and 4).

In the spectra with an applied external magnetic field (Figs. 5 and 7), energetic positions and intensities of the *fs*-components are magnetic field dependent. The Zeeman splitting is responsible for the resolution of the *fs*-components in the spectra of DPB orthorhombic (Fig. 5). In the case of DPH monoclinic the *fs*-components cannot be resolved in the spectra with an applied magnetic field (Fig. 7) due to their larger linewidths.

The field dependence of the *energies* of the *fs*-components is described by including the Zeeman term $g\mu_B\hat{\mathbf{H}}\hat{\mathbf{S}}$ in the Hamiltonian (1). As a result the equations (2b) are obtained:

$$\begin{aligned} \mathbf{B}\|\mathbf{x}^* &: E_0 = \frac{1}{3}D^* - E^* \\ & E_\pm = -\frac{1}{2}\left(\frac{1}{3}D^* - E^*\right) \pm \left(\frac{1}{4}(D^* + E^*)^2 + (g\mu_B B)^2\right)^{1/2} \\ \mathbf{B}\|\mathbf{y}^* &: E_0 = \frac{1}{3}D^* + E^* \\ & E_\pm = -\frac{1}{2}\left(\frac{1}{3}D^* + E^*\right) \pm \left(\frac{1}{4}(D^* - E^*)^2 + (g\mu_B B)^2\right)^{1/2} \\ \mathbf{B}\|\mathbf{z}^* &: E_0 = -\frac{2}{3}D^* \\ & E_\pm = \frac{1}{3}D^* \pm (E^{*2} + (g\mu_B B)^2)^{1/2} \end{aligned} \tag{2b}$$

The field dependence of the *intensities* of the *fs*-components is due to the mixing of the wavefunctions of the three spin states.

For an arbitrary orientation of the applied magnetic field transitions into all of the three spin states can be seen. In zero field generally only the transition into one of the three spin states is observable (radiative transition). When the applied magnetic field is oriented parallel to a principal axis of the *fs*-tensor, the related spin state is not mixing and two cases can be distinguished:

(i) If the principal axis belongs to the radiative component the spectra remains unchanged with an applied magnetic field.
(ii) In the other cases a Zeeman splitting into two components is observed because the *fs*-components which are optically forbidden in zero field can borrow intensity from the radiative *fs*-component. With increasing field strength the intensities of the Zeeman splitted *fs*-components approach each other. They are equal when the Zeeman splitting is large with respect to the zero field splitting (high field limit).

According to (2b) the energetic positions of the *fs*-components with an applied magnetic field are split symmetrically to the average position of their zero field energies. The distinction of the two cases (i) and (ii) allows us to assign the *fs*-components and to calculate their energies in zero field.

### *Assignment and Energetic Positions of the fs-Components in Zero Field*

For DPB orthorhombic (Fig. 5) DC 3 in ③ and DC 1 in ④ remains unchanged both in energy and intensity with an applied magnetic field (case (i)). Consequently the radiative *fs*-components belongs to the triplet spin function $t_{y'}(= t_a)$. For DPH monoclinc (Fig. 7) DC 1 in ④ and ③ and DC 2 in ③ remains unchanged. The corresponding spin functions are $t_{y'}$, $t_{z'}$ and $t_{y'}$, respectively. The assumed orientation of the *fs*-tensor as shown in Figure 9 is confirmed.

The amount of the splitting for DPB orthorhombic of DC 1, DC 2 and DC 3 with an applied magnetic field is about 0.5 $cm^{-1}$ as is expected for the Zeeman-splitting. Thus the splitted lines correspond to *fs*-components of DC 1, DC 2 and DC 3. For DC 4 the *fs*-components cannot be resolved because DC 4 is not appearing isolated in the spectra but only in superposition with DC 3.

The energetic positions of the *fs*-components with applied magnetic field allow us to determine the energies of the non-radiative *fs*-component in zero

field (case (ii)). This will be demonstrated using DC 2 in spectra ① and ③ (Fig. 5) for $B \parallel b$ and $B \parallel a$, respectively, in connection with the schemes in Figure 10.

According to Figure 5 the observed line DC 2 (radiative component) is affected by the magnetic field in both orientations $B \parallel a$ and $B \parallel b$. Thus the radiative component can be assigned to $t_c (= t_{x'})$.

In ①, $B \parallel b$, at $B = 0.27\ T$ a symmetrical splitting into two components of the same intensity was found. As for this orientation $t_b$ carries no intensity only $t_a$ and $t_c$ are contributing. From the spectrum at $B = 0.14\ T$ it can be concluded that the low energy component represents $t_c$ because its intensity is higher than that of the high energy component.

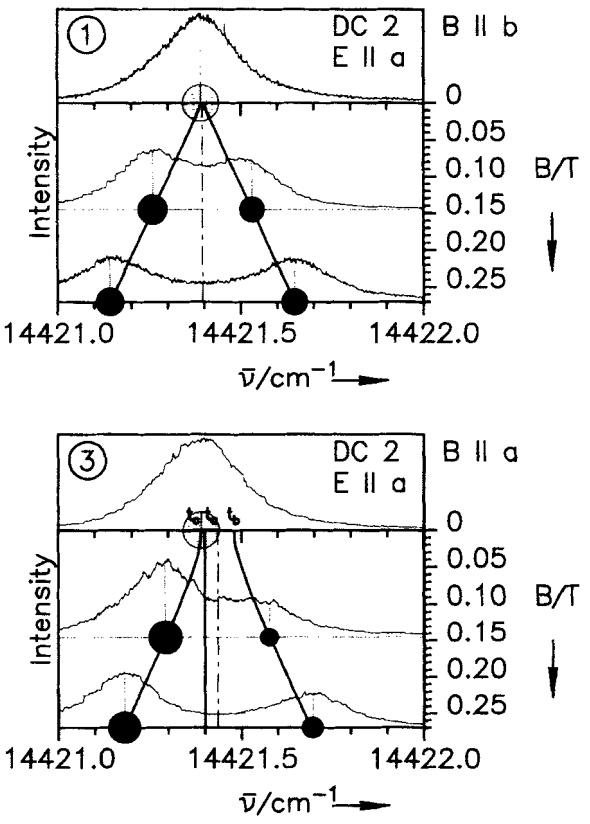


FIGURE 10 Magnetic field dependent line intensities and line positions of the fine structure components of DC 2 (labels ① and ② as in Figure 5, (a) $E \parallel a$, $B \parallel b$; (b), $E \parallel a$, $B \parallel a$. Measured lines and relative intensities (dots, schematic) for $B = 0$, $B = 0.15\ T$ and $B = 0.27\ T$ calculated line positions as a function of magnetic field strength (right hand ordinate scale).

In ③, $B \parallel a$, at $B = 0.27$ $T$ in contrast to $B \parallel b$ an asymmetrical splitting with respect to $t_c$ in zero field together with a difference in line intensities is observed. It follows that in this case the high energy component is representing $t_b$. For the *fs*-components appearing in this magnetic field orientation the high field limit for the Zeeman splitting is not achieved yet.

The energetic position of the *fs*-component $t_c$ is identical to that of the observed line in zero field. The energetic positions of the *fs*-components $t_a$ and $t_b$ in zero field are derived from the positions of the Zeeman components in high magnetic field as the averaged energies of $t_a$ and $t_c$ in ①, $B \parallel b$, and $t_b$ and $t_c$ in ③, $B \parallel a$, respectively are identical in high and zero field.

For DC 1 and DC 3 the assignment of the *fs*-components to the *fs*-tensor principal axes and the determination of the zero field energies is similar to the procedure followed for DC 2. In addition to the spectra in Figure 5 those at $E \parallel a$, $B \parallel c$ and $E \parallel b$, $B \parallel c$ (not shown) are required for the evaluation, since two splitting patterns are needed to determine the energies of the *fs*-components in zero field. A summary of the energies of all *fs*-components in zero field of DC 1, DC 2 and DC 3 are given in Table IV.

TABLE IV Energetic positions (in $cm^{-1}$), principal axes and assignment to the triplet spin states of the *fs*-components in zero field of the Davydov components DC 1, 2 and 3 of the 0-0 transition in the spectrum of DPB orthorhombic. The accuracy is due to the sum of possible errors made by the determination of the energetic positions of the *fs*-components in spectra with applied magnetic field (Fig. 5) as described in 5.2

| *DC, D* and E** | *energetic position* | *axis* | *triplet spin state* | *accuracy* |
|---|---|---|---|---|
| DC1 | 14421.35 | *b* | $t_{z^*}$ | ±0.015 |
| | 14421.28 | *a* | $t_{y^*}$ | ±0.005 |
| | 14421.27 | *c* | $t_{x^*}$ | ±0.015 |
| *D** | | | −0.075 | ±0.03 |
| *E** | | | 0.005 | ±0.01 |
| DC 2 | 14421.48 | *b* | $t_{z^*}$ | ±0.015 |
| | 14421.41 | *a* | $t_{y^*}$ | ±0.015 |
| | 14421.39 | *c* | $t_{x^*}$ | ±0.005 |
| *D** | | | −0.08 | ±0.03 |
| *E** | | | 0.01 | ±0.01 |
| DC 3 | 14422.84 | *b* | $t_{z^*}$ | ±0.03 |
| | 14422.66 | *a* | $t_{y^*}$ | ±0.01 |
| | 14422.64 | *c* | $t_{x^*}$ | ±0.03 |
| *D** | | | −0.19 | ±0.06 |
| *E** | | | 0.01 | ±0.02 |

### *fs*-Parameters $D^*$ and $E^*$

To calculate the excitonic $D^*$ and $E^*$ values from expressions (2), we have chosen the correlation $c \leftrightarrow x^*$, $a \leftrightarrow y^*$ and $b \leftrightarrow z^*$, because usually the smaller energy splitting is $2 \cdot |E|$ and the larger $|D| + |E|$. This leads to the $D^*$- and $E^*$-values listed in Table IV. The energetic ordering of the *fs*-components and the assignment to the principal axes of the *fs*-tensor is shown in Figure 11.

For the parameters $D^*$ and $E^*$ there is also one set of values available obtained from ODMR-measurements in zero field [23]. As the ODMR-signals are detected indirectly by delayed fluorescence and with crystal samples at arbitrary orientations, the $D^*$ and $E^*$ values obtained have to be considered as average on the Davydov components.

The values reported in [23] ($|D^*| = 0.049\ \text{cm}^{-1}$, $|E^*| = 0.013\ \text{cm}^{-1}$) are in reasonable agreement with those of DC 1 and DC 2 derived in this work, taking into account the different sample temperature ($T = 1.2$ K [23]), which might affect the magnitude of the *fs*-parameters, and the somehow limited accuracy of the present experiments (see Tab. IV).

It is a great advantage of the photoexcitation experiment as compared to ODMR to provide the sign of the *fs*-parameters as well. From the negative $D^*$-value and the positive $E^*$-value it follows that the *b*-axis represents the long axis of the *fs*-tensor.

### Localization of the Molecular Triplet State

In [23] also molecular $D$ and $E$ values are reported which are derived from trap signals observed in the ODMR experiments. Because $E$ is small as compared to $D$ ($|D| = 0.093\ \text{cm}^{-1}$, $|E| = 0.013\ \text{cm}^{-1}$) it is assumed that the long axis of the molecular *fs*-tensor corresponds to the direction of the polyene chain, what is in agreement with results on other polyenes [24] and indirectly supported by the sign of the excitonic *fs*-parameters $D^*$ and $E^*$ obtained above (due to $H_{exc} = 1/4\ (H_1 + H_2 + H_3 + H_4)$, where $H_1 \ldots H_4$ are

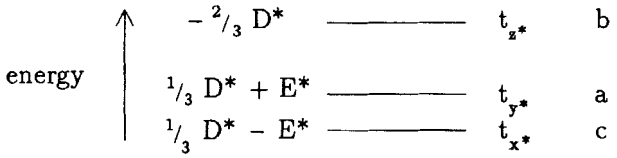


FIGURE 11 Energetic ordering of the fine structure components for the Davydov component DC 2 in zero field; DPB orthorhombic (see Tab. IV).

the molecular Hamiltonian of the four different sites in DPB orthorhombic, excitonic and molecular *fs*-parameters are correlated, see for instance [23]).

In the point-dipole approximation the average distance between the triplet spins was determined according to [25]: $\langle r \rangle \leq (3g^2\mu_B^2/4D)^{1/3}$ and with the $D$-value from above a distance of about 3 Å is derived. Considering the length of the polyene chain in DPB, which is about 6.3 Å, it must be concluded that the molecular triplet state cannot be located on the phenyl end groups but is located on the polyene chain. This conclusion is supported by results obtained from the vibronic spectra (see Chapter 6).

### 5.3. Zero-Field Intensities and Molecular Transition Moment

The aim of this chapter is to draw conclusions on the molecular transition dipole moment. It is derived from the relative intensities of the DCs in zero field measured for different polarizations of the exciting light. The zero field intensities in the spectra of the 0-0 transition result from superposition of the *fs*-components for a given polarization.

These intensities are dependent on the direction of the molecular transition moment, the direction of the molecular *fs*-tensor principal axis of the coupling triplet spin state, the polarization direction of the excitation light and the direction of the excitonic *fs*-tensor principal axes. In the special case of only one coupling triplet spin state the relative intensities are given by the expression:

$$I = \cos^2\alpha \cdot \cos^2\beta \tag{5}$$

where $\alpha$ is the angle between the polarization direction and the molecular transition moment and $\beta$ is the angle between the direction of the molecular *fs*-tensor principal axis of the coupling molecular triplet spin state and the direction of the *fs*-tensor principal axis of the excitonic triplet spin state.

For the ratio of the *total* intensities of the spectra at different polarizations, (5) can be simplified. (6) gives the expression for the total intensity ratio for $E \parallel a$ and $E \parallel b$:

$$I_{\parallel a}/I_{\parallel b} = (\mu_a/\mu_b)^2, \tag{6}$$

where $\mu_a$ is the projection of the molecular transition moment on the crystal $a$-axis and $\mu_b$ that on the $b$-axis, respectively.

In order to find the direction of the transition moment we have compared the measured intensity ratios with calculated ones when using the molecular

axes as directions for the transition moment. Because the molecular axes of the diphenylpolyenes are not clearly defined due to the molecular point symmetry (see Chapter 2) a large range of calculated values is obtained for DPB orthorhombic and DPH monoclinic (Tab. V) when considering the different possible axes as illustrated in Figure 1a for DPH monoclinic.

For DPH monoclinic nevertheless it is a clear result from the obtained intensity ratios that the transition moment cannot be in the molecular plane. The best agreement of measured and calculated values exists using the normal axis as direction for the transition moment.

For DPB orthorhombic the results are also consistent with a short axis as direction for the transition moment. But taking the affinity of the DPB molecular geometry to that of the DPH molecule into account and additional measurements in other orientations (not shown) the short axis can be excluded as possible direction for the transition moment.

Thus in both molecules (DPB and DPH) the direction of the transition moment is perpendicular to the molecular plane. It follows that the symmetry of the triplet state is $A_u$ (c.f. character table of the $C_{2h}$ point group). This is surprising because the coupling singlet state has to have the same symmetry as the triplet state and usually the symmetries of the lowest singlet states in diphenylpolyenes are $A_g$ or $B_u$ [2].

Assuming the transition to be purely electronic the $A_u$ symmetry would require a $\pi\sigma^*$ or $\pi\sigma^*$-state [2]. But these states are very high in energy [26],

TABLE V Calculated and measured total intensity ratios of the 0-0-transition spectra of DPH monoclinic and DPB orthorhombic (Fig. 3) for different polarizations in zero field. The range of calculated values is due to the uncertainty of the molecular axes according to the point symmetry of the molecules. The range of experimental values is found for different crystal samples

| | | *DPH mono.* $I_{\parallel b} : I_{\parallel c}$ | *DPB ortho.* $I_{\parallel a} : I_{\parallel b}$ |
|---|---|---|---|
| long axes | between | 1 : 13 | 1 : 8.6 |
| | and | 1 : 6400 | $1 : 10^6$ |
| short axes | between | 1 : 13 | 1 : 1.2 |
| | and | 1 : 3.2 | 12 : 1 |
| **normal axes** | between | 5.3 : 1 | 4 : 1 |
| | and | 6.7 : 1 | 5.4 : 1 |
| **experiment** | between | **2.6 : 1** | **7.3 : 1** |
| | and | **3.6 : 1** | |

and therefore the singlet-triplet coupling strength is expected to be negligible.

The further possibility of a coupling of vibrations with $B_g$ symmetry to a $B_u$ electronic transition, in order to obtain the total symmetry $A_u$, can be excluded because only vibrations with $A_g$-symmetry are observed in the measured spectra (see discussion in Chapter 6).

Thus only the assumption of molecular symmetry $C_i$ instead of $C_{2h}$, caused by the deviation of the diphenylpolyene carbon skeleton from an exact plane (see Chapter 2), can explain the direction of the transition moment perpendicular to the molecular plane. Singlet states with symmetry $B_u$ in $C_{2h}$ have the symmetry $A_u$ in $C_i$. Then a polarization direction is no longer limited to the molecular plane but can be perpendicular also for transitions into the lower singlet states.

To confirm the perpendicular direction of the transition moment the intensities of the single *fs*-components according to (5) have been calculated and compared with the measurements. For the calculation it is necessary however to know the coupling molecular triplet spin states.

The symmetry of the possible coupling spin states can be determined from the fact that the product of the symmetry of the orbital triplet state and the spin state has to be $A_u$.

In literature [27, 28] the orbital symmetry of the triplet state is assumed to be $B_u$. Then according to group theory the symmetry of the coupling spin states has to be $B_g$ and within $C_{2h}$ point group both triplet spin states $\tau_x$ and $\tau_y$ are possible ($x$ and $y$ denote molecular long and short axis).

For DPH monoclinic the calculated intensities and symmetries for the *fs*-components using $\tau_y$ as coupling triplet spin state are given in Table VI. Because the *fs*-components cannot be resolved in the spectra, in Figure 12 the total intensities of the DC for different polarizations are shown. The good agreement of calculated and measured intensities confirms $\tau_y$ as coupling molecular triplet spin state.

TABLE VI Calculated relative intensities of the *fs*-components of DC 1 and DC 2 for the 0-0 transition of DPH monoclinic in zero field and assignment to the excitonic triplet spin states $t_{n^*}$. The intensities are normalized to that of the most intensive *fs*-component $t_{y^*}$ of DC 2

| | *DC 1 ($A_u$)* | | | *DC 2 ($B_u$)* | | |
|---|---|---|---|---|---|---|
| | $t_{x^*}$ | $t_{y^*}$ | $t_{z^*}$ | $t_{x^*}$ | $t_{y^*}$ | $t_{z^*}$ |
| $\|b$ | | | 0.38 | $\sim 0$ | 1 | |
| $\|c$ | $\sim 0$ | 0.16 | | | | 0.05 |

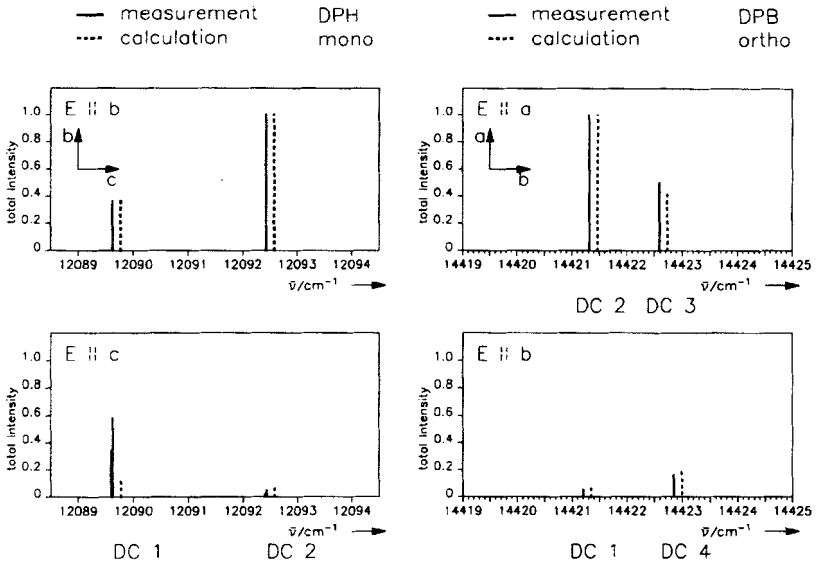


FIGURE 12 Relative intensities of the 0-0 Davydov components DC 1 and DC 2 for DPH monoclinic (left) and DC 1...4 for DPB orthorhombic (right) for different polarizations of the exciting light, schematic, measured in zero field at $T = 4.2$ K (full lines) and calculated (dotted). Experimental spectra see Figures 3 and 4.

For DPB orthorhombic the assumption of only one coupling triplet spin state does not leed to agreement between calculated and measured intensities. Only when taking $\tau_x$ as second triplet spin state into account and with similar strength as $\tau_y$ calculated and measured intensities are in good agreement (Fig. 12).

The achieved agreement of the DC intensities for both DPB orthorhombic and DPH monoclinic confirms the direction of the transition moment perpendicular to the molecular plane and thus the $A_u$ symmetry of the triplet state.

## 6. VIBRONIC SPECTRA AND DISCUSSION

In this chapter the vibronic structure of the triplet photoexcitation spectra will be considered, in particular to derive information on the localization of the molecular triplet state within the molecule. The discussion takes into account additional data obtained from ground state Raman spectra and triplet photoexcitation spectra of selectively deuterated DPH monoclinic.

Upon deuteration the energies of molecular vibrations are reduced due to the larger mass of the deuterium atoms. Therefore spectra taken on different selectively deuterated DPH monoclinic provide the means to distinguish vibrations involving different molecular subunits (polyene chain and phenyl ring modes, resp.).

Ground state Raman, singlet emission and absorption spectra of diphenylpolyenes are dominated by strong C=C (C double bond) stretching modes with energies around 1600 $cm^{-1}$, several C—C (C single bond) stretching modes at medium intensities between 1100 $cm^{-1}$ and 1300 $cm^{-1}$ which are not clearly attributed in detail yet and typical ring modes from which the mode *ring 1* (labelling of the *ring* modes according to [29]) at about 1000 $cm^{-1}$ is the strongest. The molecular vibrational modes can be attributed to one of three different classes: ring modes, chain modes and vibrations of the overall molecule. In singlet spectra, both ring and chain C=C and C—C stretching modes are observed in addition to vibrations involving the overall molecule.

A rough assignment for the triplet $T_1 \leftarrow S_0$ spectra has been made in the case of DPH [4], but it still lacks the distinction between ring and chain modes. The coarse vibronic energy and intensity pattern of the $T_1 \leftarrow S_0$ spectra resembles that of the singlet spectra with the exception of mode *ring 1* which is absent for DPH or of poor intensity for DPB.

### 6.1. Raman Spectra of Deuterated DPH Monoclinic

In Figure 13, Raman spectra of selectively ring-deuterated ($d_{10}$) and chain-deuterated ($d_6$) DPH monoclinic recorded in an energy range of 1700 $cm^{-1}$ relative to the excitation wavelength at 15450 $cm^{-1}$ (red line of a krypton ion laser) are compared with the spectrum of undeuterated DPH ($d_0$). The spectral range between 1500 $cm^{-1}$ and 1700 $cm^{-1}$ of the close lying C=C stretching modes is also given in enlarged energy scale (Fig. 13b).

For the reference spectrum of DPH-$d_0$ the assignment of typical diphenylpolyene ring and chain modes is given in Table VII according to [28]. The most prominent spectral changes for the deuterated species are the following:

- Lines R2, R4 and R6, corresponding to the *ring* modes *1*, *9a* and *19b*, respectively are strongly red-shifted for $d_{10}$ as compared to $d_0$ (by 37 $cm^{-1}$, 33 $cm^{-1}$ and 67 $cm^{-1}$, resp.) but are not displaced for $d_6$.
- Lines R7 and R8, corresponding to the C=C stretching modes *ring 8a and 8b* are similarly red-shifted in the spectrum of $d_{10}$ (by 34 $cm^{-1}$ and 29 cm, resp.) but do not appear in the spectrum of $d_6$.

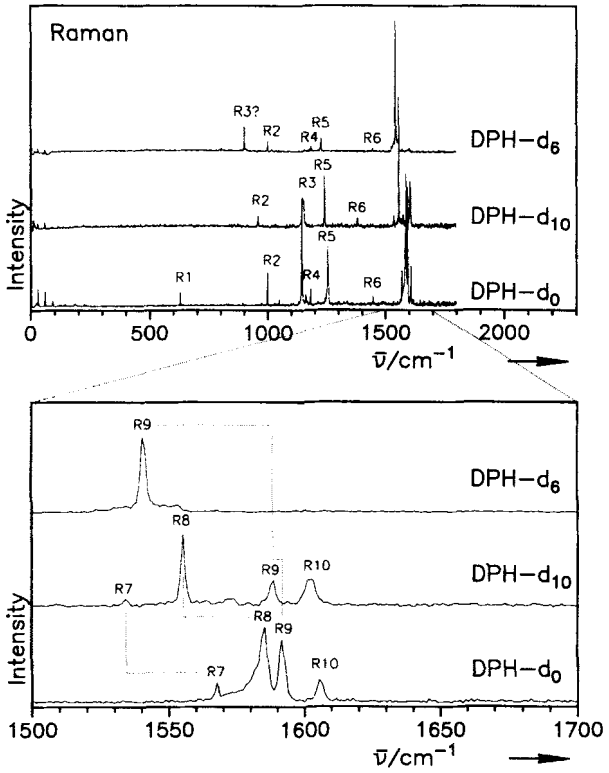


FIGURE 13 Ground state Raman spectra of selectively deuterated DPH monoclinic at $T=4.2$ K; Kr-Laser excitation at 14784 $cm^{-1}$(676.4 nm). Below, DPH-$d_0$ (undeuterated); middle, DPH-$d_{10}$ (ring deuterated); above DPH-$d_6$ (chain deuterated); energies relative to laser excitation. The energy region between 1500 $cm^{-1}$ to 1700 $cm^{-1}$ is shown separatly in enlarged scale.

TABLE VII Vibrational energies of the most prominent lines in the ground state Raman spectra at $T=4.2$ K of monoclinic DPH: undeuterated $d_0$, ring deuterated $d_{10}$ and chain deuterated $d_6$ (see Fig. 13)

| *line* | $DPH_{d0}$ | $DPH_{d10\text{-}ring}$ | $DPH_{d6\text{-}chain}$ | *assignment* |
|---|---|---|---|---|
| R1 | 619 | | | *ring 6a** |
| R2 | 996 | 959 (−37) | 999 (−03) | *ring 1** |
| R3 | 1144 | 1149 (+05) | 899 (−245) | C—C stretch chain |
| R4 | 1182 | 1149 (+05) | 1183 (+01) | *ring 9a** |
| R5 | 1254 | 1240 (−14) | 1225 (−29) | chain-ring stretch |
| R6 | 1446 | 1379 (−67) | 1445 (−01) | *ring 19b** |
| R7 | 1568 | 1534 (−34) | | C=C stretch *ring 8b* |
| R8 | 1585 | 1556 (−29) | | C=C stretch *ring 8a* |
| R9 | 1592 | 1589 (−03) | 1542 (−50) | C=C stretch chain |

*Labelling of the ring-modes according to Wilson [29].

The amounts of red shifts for the *ring* modes, *1*, *8a*, *8b*, *9a* and *19b*, respectively, are in accord with literature data obtained for deuterated benzene [30].

- Line R5 corresponding to a chain-ring-stretch mode is red shifted for both $d_{10}$ and $d_6$ but by different amounts (14 $cm^{-1}$and 29 $cm^{-1}$, resp.).
- In contrast, line R9 and R10 corresponding to C═C chain stretching modes are heavily red shifted for $d_6$ (by 50 $cm^{-1}$ and 53 $cm^{-1}$, resp.), but only slightly displaced (by 3 $cm^{-1}$) for $d_{10}$.

From these findings the selective deuteration is proven clearly and the distinction of polyene chain and phenyl ring modes via the deuteration effect is possible.

### 6.2. Triplet Photoexcitation Spectra of Deuterated DPH Monoclinic

In Figure 14, photoexcitation spectra of DPH-$d_{10}$ and DPH-$d_6$ are shown together with spectra of DPH-$d_0$ (dotted lines). To allow for comparison of the relative vibrational energies, the spectra are normalized in energy scale to the 0-0 transition of DPH-$d_0$ . The actual 0-0 line positions of DPH-$d_{10}$ and DPH-$d_6$ are equal and blueshifted by 28$cm^{-1}$. The absolute energies of 0-0 transition and predominant vibronic lines (C—C and C═C stretching modes) are listed in Table VIII.

The spectrum of DPH-$d_{10}$ (ring-deut.) shows a similar vibronic structure as that of DPH-$d_0$ whereas the vibrational pattern of DPH-$d_6$ (chain-deut.) is clearly different. For DPH-$d_6$ line 11 is strongly reduced in energy by 47 $cm^{-1}$ but the C—C stretching modes lines 3, 4 and 5 have disappeared.

Because of the similarity of the triplet photoexcitation spectra of DPH-$d_{10}$ and DPH-$d_0$ on one hand and the difference between the spectra of DPH-$d_6$ and DPH-$d_0$ on the other hand, the vibrational lines dominating the spectra of DPH-$d_0$ can be attributed to (C—C and C═C-stretching) chain modes.

### 6.3. Triplet Photoexcitation Spectra of DPB

Because the intensity dependence of the vibronic lines in the triplet photoexcitation spectra of both DPB and DPH on the polarization direction of the excitation light is the same as for the 0-0 lines it is assumed that all the vibronic modes have $A_g$ symmetry. In the singlet spectra the most prominent lines have $A_g$ symmetry as well [31]. Therefore the vibrational assignments made in literature [28] are transferred to our spectra.

Because the vibronic pattern of the triplet photoexcitation spectra of DPB (Fig. 2) are very similar to those of DPH ( Fig. 14 and [4]), the assignment of

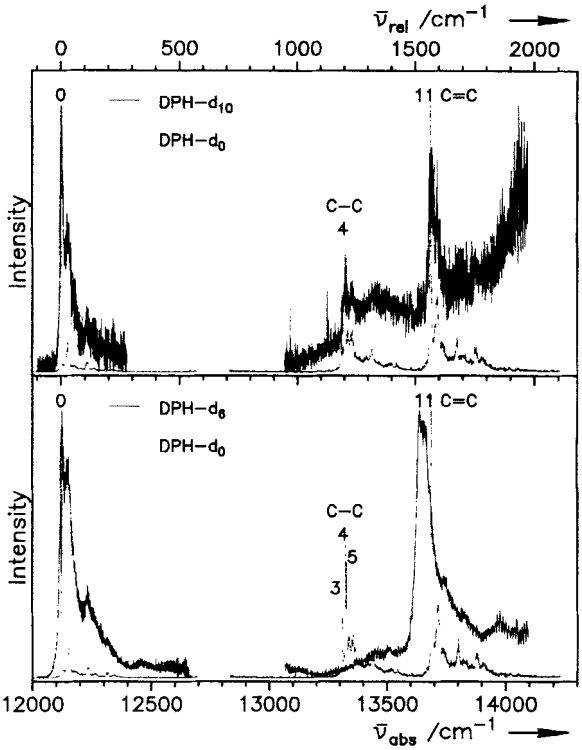


FIGURE 14 Comparison of the vibronic structure in photoexcitation spectra of selectively deuterated and undeuterated DPH monoclinic at $T = 20$ K. Above: full line, DPH-$d_{10}$ (ring deuterated); dotted, DPH-$d_0$; below: full line, DPH-$d_6$ (chain deuterated); dotted, DPH-$d_0$. The spectra are normalized in energy to the identical 0-0-line position of DPH-$d_6$ and -$d_{10}$, relative vibronic energies are given in the upper scales.

TABLE VIII Absolute energies of the 0-0-transitions in the measured triplet photoexcitation spectra at $T = 20$ K of monoclinic DPH: $d_0$ (nondeuterated), $d_{10}$ (ring deuterated) and $d_6$ (chain deuterated) and relative vibronic frequencies of the C—C stretching (lines 3, 4, 5) and C=C stretching modes (line 11) (Fig. 14). The lines are labelled the same as for DPB (Tab. II). In brackets the deviations from the values of DPH-$d_0$ are given. All data in cm$^{-1}$

| *line* | *DPH-$d_0$* | *DPH-$d_{10}$* | *DPH-$d_6$* |
|---|---|---|---|
| 0 | 12092 | 12120 (+28) | 12120 (+28) |
| 3 | 1189 | | |
| 4 | 1205 | 1202 (−3) | |
| 5 | 1209 | | |
| 11 | 1567 | 1565 (−2) | 1518 (−47) |

the C—C and C=C stretching modes to chain modes for DPH (see above) also is adoped for DPB. The assignment of line 11 is additionally supported by the transient triplet $T_1$-Raman spectra in [28].

In contrast to the triplet photoexcitation spectra of DPH where no ring modes are observed, two typical ring modes appear in the spectra of DPB (line 3 and 4) at energies of 595 $cm^{-1}$ and 980 $cm^{-1}$, respectively. They correspond to modes which are pronounced in Raman spectra and attributed to *ring 6a* and *ring 1*, respectively [28] (labelling according to Wilson [29]).

The lack of ring modes with energies larger than 1000 $cm^{-1}$ in the triplet photoexcitation spectra of both DPB and DPH and the very weak intensity of the modes *ring 6a* and *ring 1* in the spectra of DPB clearly proves that the molecular $T_1$ excitation energy is localized mainly on the polyene chain. The tentative conclusion drawn in chapter 5.2. from the molecular *fs*-parameters $D$ and $E$ is consistent with this finding.

The two lines (1 and 2, Tab. II) with energies of 144 $cm^{-1}$ and 226 $cm^{-1}$ in the spectra of DPB monoclinic (Fig. 2a) and 156 $cm^{-1}$ and 230 $cm^{-1}$ in that of DPB orthorhombic (Fig. 2b), respectively, fit very well with energies of symmetric planar bending modes of the overall DPB molecule (157 $cm^{-1}$ and 232 $cm^{-1}$) measured in ground state Raman [31]. The relative strong intensity of those lines in the triplet photoexcitation spectra is a hint for the strong coupling of these modes with the electronic transition, possibly originating in a planar distortion of the molecule.

## 7. CONCLUSIONS

From an analysis of the photoexcitation spectra of the $T_1$ state in DPB and DPH single crystals without and with an applied magnetic field we have been able to analyze the Davydov components in the excitonic spectra. The direction of the molecular transition moment in shown to be perpendicular to the molecular plane and consequently the symmetry of the $T_1$ state is $A_u$. The vibrational structure of the spectra of crystals with ring- and chain-deuterated molecules gives clear evidence for location of the triplet state on the polyene chain and not on the phenyl rings.

### *Acknowledgement*

Purification, analysis and crystal growth were performed by the staff of our Kristalllabor. The syntheses of the deuterated compounds have been carried

out by W. Tuffentsammer. We are grateful to S. Henkel and Prof. J. J. Stezowski for structure analysis and Dr. E. J. J. Groenen for helpful discussions. Financial support has been provided by Deutsche Forschungsgemeinschaft.

## References

[1] B. S. Hudson and B. E. Kohler, *Annul. Rev. Phys. Chem.*, **25**, 437 (1974).
[2] B. S. Hudson, B. E. Kohler and K. Schulten, in: *Excited States*, **6** (Ed. E. C. Lim, Academic Press, N.Y. 1982), 1–95.
[3] J. K. Duchowski and B. E. Kohler, *Mol. Cryst. Liq. Cryst. Sci. Technol.*, Sect. **A 256**, 449 (1994).
[4] V. Weiss, H. Port and H. C. Wolf, *Chem. Phys. Lett.*, **192**, 289 (1992).
[5] W. Drenth and E. H. Wiebenga, *Rev. Trav. Chim. Pays-Bas*, **72**, 39 (1953).
[6] T. Hall, S. M. Bachrach, C. W. Spangler, L. S. Sapochak, C. T. Lin, H. W. Guan and R. D. Rogers, *Acta Cryst.*, **C45**, 1541 (1989).
[7] G. Heinrich, G. Holzer, H. Blume and D. Schulte-Frohlinde, *Z. Naturforsch*, **25B**, 496 (1970).
[8] J. P. Aime, V. Ern, J. L. Fave and M. Schott, *Mol. Cryst. Liq. Cryst.*, **46**, 169 (1978).
[9] J. Hengstenberg and R. Kuhn, *Z. Krist*, **75**, 301 (1930).
[10] C. Ross, Unpublished results.
[11] A. S. Davydov, *Theory of Molecular Excitons*, Plenum Press, N.Y. (1971).
[12] D. F. Evans, *J. Chem. Soc.*, 1351 (1957).
[13] D. F. Evans and J. N. Tucker, *J. Chem. Soc. Faraday Trans.*, **II 68**, 174 (1972).
[14] V. Ramamurphy, J. V. Caspar, D. R. Corbin, B. D. Schlyer and A. H. Maki, *J. Phys. Chem.*, **94**, 3391 (1990).
[15] E. G. Cox, D. W. J. Cruickshank and J. A. S. Smith, *Proc. Roy. Soc.* (London) **A 247**, 1 (1958).
[16] R. Kopelman, *J. Chem. Phys.*, **47**, 2631 (1967).
[17] R. M. Hochstrasser, In: *Spectroscopy*, *Phys. Chem. Ser.2*, **3** (Ed. D. A. Ramsay, Butterworths, London, 1976), 1–36.
[18] H. Port, D. Rund and H. C. Wolf, *Chem. Phys.*, **60**, 81 (1981).
[19] K. Mistelberger and H. Port, *Mol. Cryst. Liq. Cryst.*, **57**, 203 (1980).
[20] U. Doberer, H. Port and H. Benk, *Chem. Phys. Lett.*, **85**, 253 (1982).
[21] P. Avakian and R. E. Merrifield, *Mol. Cryst.*, **5**, 37 (1968).
[22] H. Sternlicht and H. M. McConnell, *J. Chem. Phys.*, **35**, 1793 (1961).
[23] Y. Teki, J. U. von Schütz, H. Wachtel, V. Weiss, H. C. Wolf, *Chem. Phys. Lett.*, **225**, 124 (1994).
[24] J. Frick, *Thesis* (Universität Stuttgart, 1992).
[25] K. Scheffler and H. B. Stegmann, *Elektronenspinresonanz*, (Springer, Berlin, 1970), 242.
[26] M. A. C. Nascimento and W. A. Goddard, III *Chem. Phys.* **36**, 147 (1979).
[27] E. J. J. Groenen, Private communications.
[28] R. Wilbrandt, W. E. L. Grossmann, P. M. Killough, J. E. Bennett and R. E. Hester, *J. Phys. Chem.*, **88**, 5964 (1984).
[29] E. B. Wilson, Jr. *Phys. Rev.* **45**, 706 (1934).
[30] G. Varsany, *Assignments for Vibrational Spectra of Seven Hundred Benzene Derivatives* (Wiley, N.Y) (1974).
[31] B. M. Pierce and R. R. Birge, *J. Phys. Chem.*, **86**, 2651 (1982).